Supporting information for "Chemical and Steady-State Kinetic Analyses of a Heterologously Expressed Heme-Dependent Chlorite Dismutase"

J.L. DuBois and B.R. Streit

(1) Protein expression optimization. For optimization of soluble protein production, cells were inoculated 1:100 into 50 mL fresh LB-kanamycin and grown to an optical density of 0.5 (600 nm) at varying temperatures (15-37 °C). The extent of uninduced protein expression was assessed by SDS polyacrylamide gel electrophoresis (SDS-PAGE) of whole cells over time. The cell optical density, temperature, and amount of IPTG added were then varied, over 0.2-0.7, 15-37 °C, and 0.1-1 mM respectively (data not shown). SDS-PAGE was used to screen for the maximal production of a ~30kDa protein (approximate Cld subunit molecular weight) in the soluble fraction. Subsequently, the effects of added heme or the heme precursor 5-aminolevulinic acid on the activity and approximate heme stoichiometry of the product were assessed. Crystalline hemin (Strem Chemicals) was added to final concentrations ranging from 10-90 μM and the activity and heme:protein stoichiometry determined for the soluble fractions of lysed cells.

(2) Isoelectric focusing. The isolectric points of recombinant and native Cld were determined using isoelectric focusing polyacrylamide gel electrophoresis (IEF-PAGE) on a pH 3.0-10.0 gradient gel (Bio-Rad). The gel was run 60 min at 100 mA, 60 min at 250 mA, and 30 min at 500 mA. Isoelectric focusing standards on the same gel (pIs labeled, Bio-Rad) were used to generate a curve of pI versus migration distance, from which the unknown pIs were determined. The gel for recombinant Cld is pictured here.

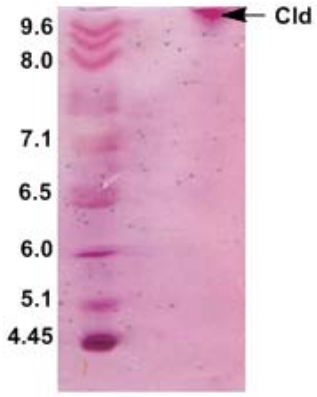

(3) Determination of ClO_2^-:O_2 reaction stoichiometries. Residual ClO_2^- was measured via iodometric titration and O_2 measured by Clark electrode, as described in the text. The following table gives results for a variety of initial chlorite concentrations tested:

Table S1. Stoichiometry of chlorite dismutated versus O_2 evolved, at various values of [chlorite]

[Chlorite] (μM)	ClO_2^- dismutated/O_2 evolved	Error
85	1.039117	0.07
95	0.96	0.06
145	1.030269	0.03
185	1.08	0.07
205	1.07	0.04
260	0.996926	0.04
530	1.040964	0.08
885	1.080748	0.08
925	1.05	0.03
1700	1.02	0.1
1740	0.96467	0.07

Errors are computed as the standard deviation of at least three independent measurements at a particular chlorite concentration. All initial rates were determined in a 100 mM potassium phosphate buffer at pH 6.8 at 4 °C.

(4) Inhibitory effects of chloride.

Initial rates of reaction vs. [ClO_2^-] (ranging from 0 – 1700 μM) were measured in the presence of a fixed amount of Cl^- ranging from 0 – 200 mM. **Figure S1**: The initial rate data (referenced to heme concentration) for each Cl^- concentration were fit to the Henri-Michaelis-Menten equation of the form: $v/[E] = k_{cat}[ClO_2^-]/(K_{app} + [ClO_2^-])$, where [E] = [heme] in Cld The catalytic parameters k_{cat} and K_{app} were determined for each [Cl] are shown in **Table S2**. All errors are determined from the standard deviation of at least three independent trials under one [Cld_{heme}], [ClO_2^-], and [Cl^-]. **Figure S2**: The reciprocal of the initial rate data (1/v) was plotted against $1/[ClO_2^-]$. The linearized data are fit to the Linweaver-Burke equation $[E]/v = (K_{app}/k_{cat})(1/[ClO_2^-]) + 1/k_{cat.}$ From the pattern of lines intersecting to the left of the y-axis and below the x-axis, it was determined that Cl^- acted as a hyperbolic mixed type inhibitor[‡] **Figure S3**: Replots of 1/Δslope and 1/Δintercept (where the change is measured relative to a no-chloride plot) versus 1/[chloride] were generated from the data in **Figure S2**. Taking into account Cl^-'s ability to bind to E or ES to form EI or ESI, the equation describing hyperbolic mixed type inhibition is of the form: $v/k_{cat} = [ClO_2^-]/((K_{app}(1+([Cl^-](\alpha-\beta)/(\beta[Cl^-]+\alpha K_i))) + [ClO_2^-](1+([Cl^-](1-\beta)/(\beta[Cl^-] + \alpha K_i))))$.[‡] This yields equations for $1/\Delta slope = (\alpha K_i k_{cat}/(K_s(\alpha-\beta)))(1/[Cl^-]) + \beta k_{cat}//(K_s(\alpha-\beta))$ and $1/\Delta intercept = (\alpha K_i k_{cat}/(1-\beta))(1/[I]) + \beta k_{cat}/(1-\beta)$.(Segal) From the linear fits to the data in **Figure S3**, values of $\alpha = 0.425$, $\beta = 0.484$, and $K_I = 225$ mM were determined where Δslope y-intercept $= \beta k_{cat}/(K_s(\alpha-\beta))$, Δ intercept y-intercept $= \beta k_{cat}/(1-\beta)$ and the intersection point of the two lines $= -\beta/(\alpha K_i)$.[‡]

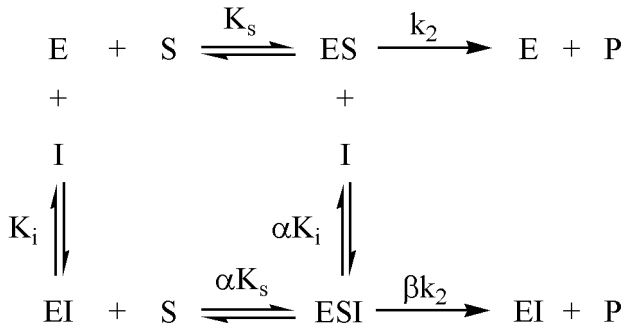

In order to better understand whether the effects due to chloride were anion-specific, or whether they might be attributed simply to the effects of ionic strength, enzyme activity in increasing amounts of chloride and triflate ($CF_3SO_3^-$) was measured. The amount of activity relative to that in the absence of any added anion was plotted versus [anion] (**Figure S4**) as a dose-response curve. Triflate is a large anion that is known to coordinate only weakly to metals. Hence, we expected it would interact minimally with the heme containing active site. As shown in **Figure S4**, however, triflate had an even greater effect on enzyme activity than chloride. Hence, the effects due to chloride are likely not simply due to increases in ionic strength.

[‡] Segel, Irwin H., *Enzyme Kinetics: Behavior and Analysis of Rapid Equilibrium and Steady-State Enzyme Systems*, Wiley-Interscience, Edition 1, 1993, Chapter 4, ISBN 0-471-30309-7

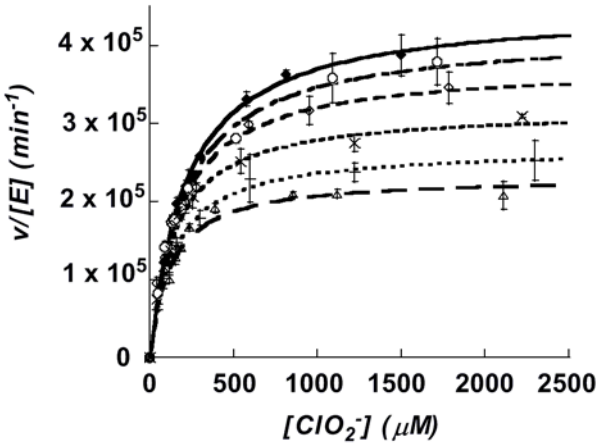

Figure S1: Overlay of the Michaelis Menten plots of Cl^- inhibition. 0 mM Cl (——— , ♦); 20 mM Cl (— — —, ○); 50 mM (— — — — —, ◊), 100 mM Cl^- (- - - - - - - -, X); 150 mM Cl^- (· · · · · · · · · ·, +); 200 mM Cl^- (— — — — —, Δ).

Table S2: Catalytic constants of ClO_2^- dismutation in the presence of Cl^-.

$[Cl^-]$ (mM)	$K_{m\ (app.)}$ (μM)	$k_{cat\ (app.)}$ (x 10^5) (min^{-1})
0	212 ± 12	4.50 ± 0.08
20	202 ± 14	4.2 ± 0.1
50	172 ± 15	3.76 ± 0.1
100	144 ± 10	3.20 ± 0.07
150	138 ± 8	2.70 ± 0.06
200	118 ± 17	2.32 ± 0.08

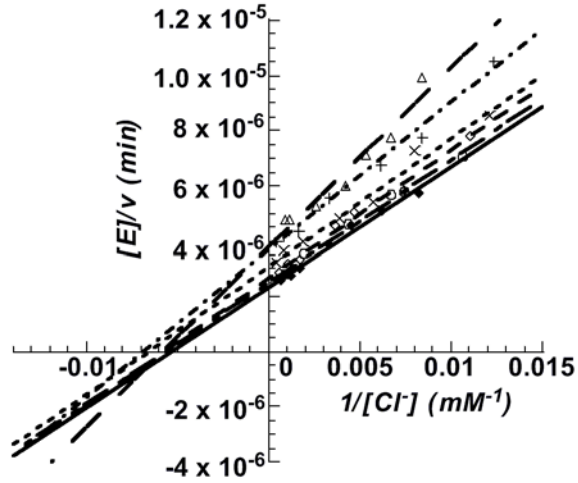

Figure S2. Lineweaver Burke plot of Cl^- inhibition. 0 mM Cl^- (——, ♦); 20 mM Cl^- (— — — —, ○); 50 mM Cl^- (— — — — —, ◊), 100 mM Cl^- (- - - - - - - -, X); 150 mM Cl^- (· · · · · · · · · ·,+); 200 mM Cl^- (— — — — —, Δ).

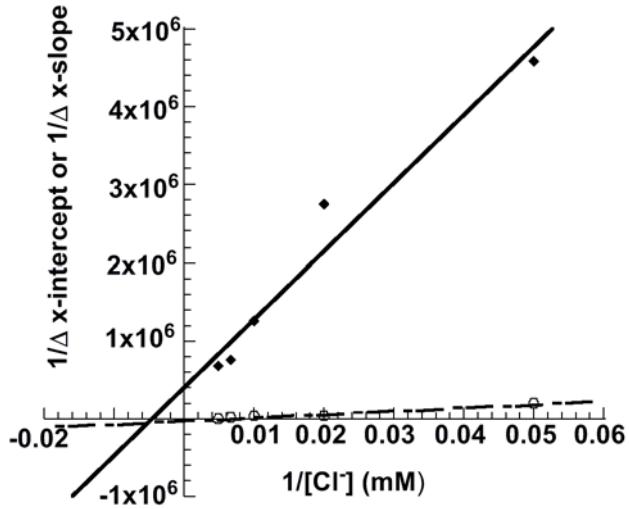

Figure S3: 1/Δslope and 1/Δintercept replots of Cl^- inhibition reciprocal data. 1/Δ intercept values (♦, solid line) 1/Δ slope values (○,dashed line).

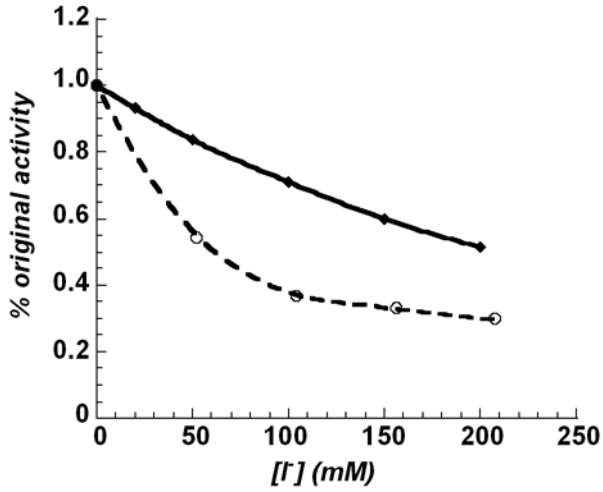

Figure S4: A dose response curve was measured to determine inhibition of Cld activity by either Cl^- (—— , ♦) or triflate anion (OTf^-) ((- - - - - - - , ○). In the presence of a normally saturating amount of ClO_2^- (2200 μM) progress of reaction curves were measured in increasing concentrations of salts (either Cl^- ion from NaCl or by triflate ion from sodium triflate) using a Clark type oxygen electrode as described in the experimental section. Points are fit with a smooth curve for ease of visualizing trend.

(5) Guaiacol protection against inactivation. In order to determine the extent to which guaiacol could protect the enzyme from chlorite-dependent inactivation, samples of enzyme (210 nM heme) were incubated with chlorite and increasing quantities of guaiacol.
A chlorite:heme ratio of 5.0 x 10^4 was used in each case. This amount of chlorite is slightly above the extrapolated turnover number for the enzyme (1.7 x 10^4 molecules of chlorite per heme; see text). (Note that the enzyme does have a small amount of residual activity at this chlorite concentration, as indicated in **Figure 6**, however, potentially due to product protection by Cl^-.) Specific activities were determined via monitoring the change in O_2 concentration using a Clark type oxygen electrode as described in the experimental section. By comparing the guaiacol incubated samples against a control sample (no guaiacol or chlorite in initial incubation before buffer exchange) the % activity remaining of each sample could be determined; in effect this is a measure of the amount of enzyme inactivated during the initial chlorite

incubation. Concentrations of guaiacol ranging from 0 – 3500 mM were tested with final guaiacol:heme ratios ranging from 0 – 16600. The plot indicates that the effect of guaiacol saturates at relatively low concentrations, e.g., by ~500 mM (~2380 equivalents per heme). Hence, at the amount of guaiacol used in generating **Figure 6** in the text (600 μM), its effect should be as great as possible.

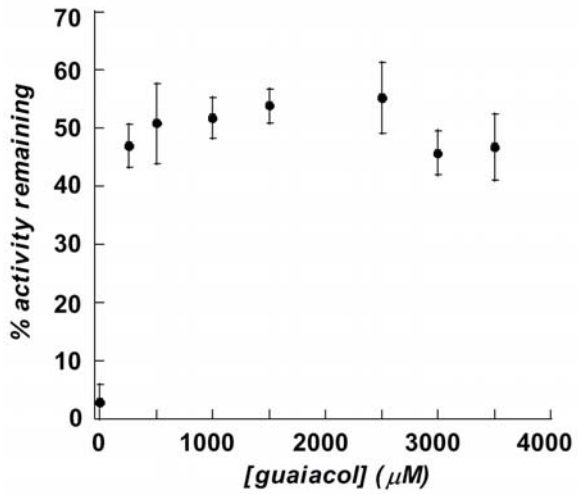

Figure S5: Dose response curve showing guaiacol's prevention of suicide inactivation of Cld.